CONTINUAL AND MOLECULAR-DYNAMIC MODELING OF PHASE TRANSITIONS DURING LASER ABLATION

A.A. SAMOKHIN[1], V.I. MAZHUKIN[2,3], A.V. SHAPRANOV[2,3], M.M. DEMIN[2], P.A. PIVOVAROV[1,3]

[1]Prokhorov General Physics Institute, RAS

[2]M.V. Keldysh Institute of Applied Mathematics, RAS, Moscow, Russia
e-mail: vim@modhef.ru

[3]National Research Nuclear University MEPhI, Moscow, Russia

Summary. Different theoretical methods including continual and molecular dynamic treatments of nonequilibrium phase transitions during laser ablation are discussed on the basis of several recent and earlier investigations. Attention is attracted, in particular, to some discrepancies in description of vaporization and explosive boiling processes.

1 INTRODUCTION

Laser ablation of condensed matters results in various phase transitions which can be dealt with different theoretical methods including continual, kinetic, molecular dynamic (MD) and other approaches. In the first of them one uses together with differential equations of motion also an equation of state which defines relations between equilibrium (or quasiequilibrium) thermodynamic parameters of the considered system. Such description is not complete because, in particular, some additional information is needed about non-equilibrium features of the first order phase transitions. This information concerns, in particular, boundary conditions at the moving phase fronts in the Stefan-like continual model of melting and vaporization processes as well as superheating limits of the considered metastable states and evolution of the states during its fast heating. Such questions do not arise in MD simulations which give more complete picture of the nonequilibrium phase transitions. On the other hand MD calculation results do not contain explicit information on thermophysical parameters which appear in the corresponding continual approach and additional procedures are needed to obtain this information.

In the present paper some results of recent and earlier investigations[1-12] are analyzed to clarify its consistency and discrepancies. In section 2 some general remarks are given on continual description of the first order phase transitions. Section 3 and 4 are devoted, respectively, to description of melting and vaporization during fast matter heating in the framework of continual and MD approaches. Concluding remarks are given in the final section 5.

2 CONTINUAL DESCRIPTION OF THE FIRST ORDER PHASE TRANSITIONS

First of all it should be reminded that the phase transitions are nonequilibrium processes except for the cases where they are infinitely slow with infinitely small mass, momentum and

2010 Mathematics Subject Classification: 80A22, 74A25, 82C21.
Key words and Phrases: Continuum and Atomistic Models, Phase Transformations, Overheated Metastable States, Laser Action.

energy fluxes across the phase boundaries. In such quasi-equilibrium processes different phase states are practically in equilibrium at the same temperature. If the process is not slow then the phase state temperatures are not equal and it is necessary to use the full set of continual differential equations for mass, momentum and energy fluxes to describe properly the phase transition process under consideration.

The simplest approach of the kind was realized as early as in XIX century by Stefan and others[13,14] who used heat conduction equation to analyze melting-freezing (solidification) process. This well-known Stefan problem is nonlinear even if all thermophysical parameters are temperature independent. This is due to moving phase transition front where Stefan boundary conditions are formulated:

$$x = \Gamma_{s\ell}(t): \qquad \lambda_s(T)\frac{\partial T_s}{\partial x} - \lambda_\ell(T)\frac{\partial T_\ell}{\partial x} = \rho_s L_m \upsilon_{s\ell} \tag{1}$$

$$T_{s\ell} = T_s = T_\ell = T_m, \tag{2}$$

In the classical Stefan problem phase front velocity can be considerably higher than sound velocity[6,15] and for this reason one should consider the phase transition problem in more general formulations[16-18]. However, some important questions about superheating (supercooling) limits or generalized boundary conditions cannot be answered in the continual approach framework. The same limitations, to some extent, are also pertinent to different forms of continual approach such as phase field model or others (see, e.g.,[19,20]) which are not considered here.

The simplest vaporization model is also based on the Stefan-like approach with appropriate boundary conditions on the evaporating surface (see, e.g.,[6,15,21] and references therein). The model is discussed in some details in sec. 4 where a comparison between continual and MD calculation results is also given.

Nonequilibrium nature of laser ablation is not only due to violations of phase equilibrium in irradiated matters. At sufficiently high laser intensities in irradiated metals electron temperature can significantly exceed lattice (ion) temperature. In analogy with plasma physics[22,23] in this case two-temperature model is used based on two separate heat conduction equations for electron and lattice (ion) interacting subsystems.[24-26] Electron heat conduction equation is also used in MD modeling of metal ablation.[27-30]

3 MELTING TRANSITION

Metastable overheated and supercooled states are inherent in all mechanisms of melting and solidification, and therefore for the theoretical and experimental studies fundamental problems, in which the solid can be overheated and liquid can be supercooled are of special interest. Although certain relationship of processes of melting and solidification exists the problem of supercooled liquids during solidification was more fully investigated,[31-33] primarily experimental, compared to the superheated states in solids.

In recent years, experimental implementation of overheated metastable states in solids was observed at high power pulsed influences in shock-wave experiments[34, 35] nanosecond electrical explosion of conductors,[36, 37] and laser irradiation.[38, 39]

A theoretical analysis of the dynamics of phase transitions of the first kind leads to a different versions of Stefan problem, [40, 41] by which in mathematical physics mean a wide class of problems with moving boundaries described by equations of parabolic or elliptic

types. In a sufficiently general statement, but without hydrodynamic processes, Stefan problem can be reduced to a boundary value problem for quasi-linear parabolic equation with piecewise continuous coefficients which have discontinuities of the first kind on the previously unknown moving surfaces. In the case of laser action processes of heterogeneous melting / crystallization and evaporation are described in the framework of a combined version of Stefan problem,[41] in which melting - hardening described by the classical Stefan problem, and the evaporation in the framework of single-phase version with movable interphase boundaries $x = \Gamma_{s\ell}(t)$ и $x = \Gamma_{\ell\upsilon}(t)$:

$$\left[\frac{\partial(\rho H)}{\partial t} = \frac{\partial}{\partial x}\lambda(T)\frac{\partial T}{\partial x} - \frac{\partial G}{\partial x}\right]_k, \quad H = C_p(T)T, \quad k = s,\ell \tag{3}$$

$$\left[\frac{\partial G}{\partial x} + \kappa(\rho,T)G = 0\right]_k, \quad G(t) = G_0\, exp\left(-\left(\frac{t}{\tau}\right)^2\right) \tag{4}$$

$$x_0 < x < \Gamma_{s\ell}(t) \bigcup \Gamma_{s\ell} < x < \Gamma_{\ell\upsilon}(t) \qquad -\infty < t < \infty$$

In the classic version of the Stefan problem for describing phase transitions melting - crystallization at the interface $x = \Gamma_{s\ell}(t)$ are used conditions (1), (2).

On evaporating surface $x = \Gamma_{k\upsilon}(t)$ as the boundary conditions are used 3 conservation laws:

$$x = \Gamma_{k\upsilon}(t): \quad \rho_\kappa \upsilon_{k\upsilon} = \rho_\upsilon(\upsilon_{k\upsilon} - u), \quad p_k + \rho_\kappa \upsilon_{k\upsilon}^2 = \rho_\upsilon(\upsilon_{k\upsilon} - u)^2, \quad \lambda_k(T)\frac{\partial T_k}{\partial x} = \rho_k L_\upsilon \upsilon_{k\upsilon}$$

$$G_k = A(T_k)G(t) \tag{5}$$

The values that characterize the nonequilibrium of surface evaporation, are determined by the ratios on the external side of the Knudsen layer by Crout model[42, 43].

$$T_\upsilon = \alpha_T(M)T_k, \quad \rho_\upsilon = \alpha_\rho(M)\rho_{sat}, \quad P_\upsilon = \alpha_T(M)\,\alpha_\rho(M)\,P_{sat}(T_k)$$

$$M = \frac{u_\upsilon}{u_{sound}}, \quad u_{sound} = (\gamma R T)^{1/2}, \quad P_{sat}(T_k) = P_b\, exp\left[\frac{L_v}{R_\mu}\left(\frac{1}{T_b} - \frac{1}{T_k}\right)\right], \tag{6}$$

$$\rho_{sat} = P_{sat}(T_k) * (R_\mu T_k)^{-1};$$

α_T, α_ρ are the Crout coefficients, M is the Mach number at the outer side of the Knudsen layer, ρ_{sat}, P_{sat} are the density and pressure of the saturated vapor, P_b, T_b, are the equilibrium boiling pressure and temperature, T_υ, ρ_υ, P_υ are the vapor temperature, density and pressure, u, u_s - gasdynamical velocity of vapor flow and the speed of sound. At $M = 1$: $T_\upsilon = 0.633\, T_\ell$, $\rho_\upsilon = 0.328\,\rho_{sat}$. $A(T_k)$ - absorptivity of surface.

In [44,45] was considered the impact of the laser with nanosecond duration $\tau = 40\, ns$, with intensity of $G_0 = 10^7 W\, cm^{-2}$ and wavelength of $\lambda_L = 1.06\,\mu m$ to the target of the superconducting ceramics ($YBa_2Cu_3O_{7-X}$) with thermophysical and optical parameters

$$T_m = 1300^{\circ}K, \quad T_\upsilon = 2000^{\circ}K, \quad C_p = 0.5\ J/g\,K,$$

$$\lambda = 3 \cdot 10^{-2}\ W/cmK, \quad \rho = 5.9 gcm^{-3}, \quad L_m = 2.5 \cdot 10^{2}\ J/g, \quad L_\upsilon = 6 \cdot 10^{3}\ J/g,$$

$$A(T_k) = 0.8, \quad \alpha = 10^{4}\ cm^{-1}$$

Mathematical modeling using a model (1) - (5) shown that, Fig. 1-3, the main features of a short and ultrashort influence on metals and ceramics are associated with high speed and volumetric nature of release of energy of the laser pulse.

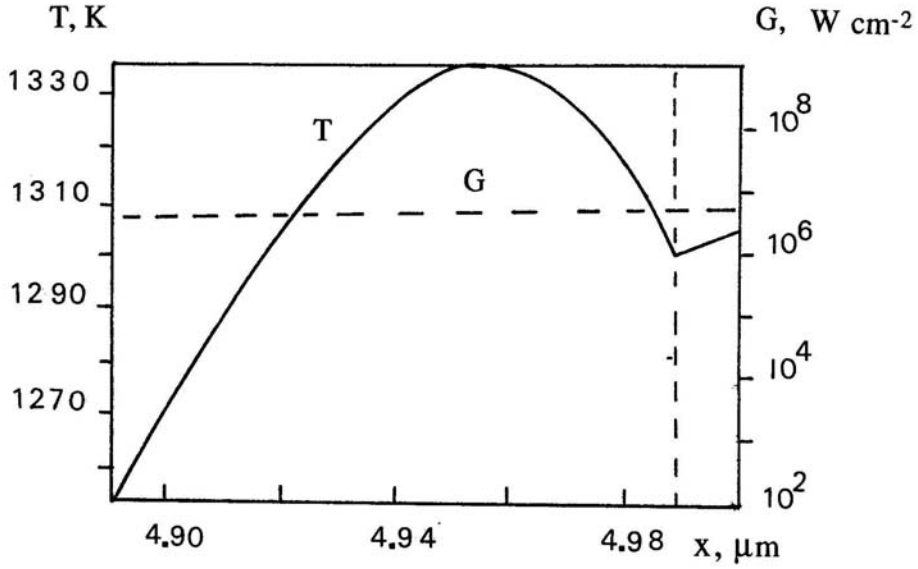

Fig.1. The spatial temperature profile (solid line) *T(x)* and intensity of the radiation (dashed line) *G(x)* in the initial moments of melting. The vertical line corresponds to the position of the interface $x=\Gamma_{kv}(t)$.

High speed of heating of condensed medium causes fast phase transformation of matter characterized by the transfer through the phase boundaries of powerful mass and energy flows. Removal the energy by the flow of matter in conjunction with the volumetric mechanism of release of energy of laser radiation can cause overheating of interface surface to temperatures far exceeding equilibrium values of melting T_m and evaporation T_b. Due to the same reasons, near the irradiated surfaces in the solid and liquid phases are formed regions of temperature maxima, Fig. 1, 2. In this case, the maximum overheat of solid phase of superconducting ceramics with respect to temperature T_m was 150°K, and the liquid - a few hundred degrees. With these assumptions, the lifetime of metastable states, respectively, are tens and hundreds of nanoseconds. Metastability of solid phase leads to the dominance of the melting process, which together with the reduction of influence of crystallization and evaporation increases in 5 - 6 times the lifetime of the liquid phase Fig.3.

Transition to the region of ultrashort influence associated with a number of qualitative changes. The rate release of energy in the pico- femtosecond range increases by several orders of magnitude. Slow exchange of energy between electrons and the lattice contributes to the appearance of strong thermodynamic nonequilibrium $T_e >> T_{ph}$. High thermal conductivity of the heated electron gas leads to a significant increase of region of volumetric release of energy

after the laser pulse. As a result the high degree of overheating of interface surfaces and near-surface layers in solid and liquid phases is realized.

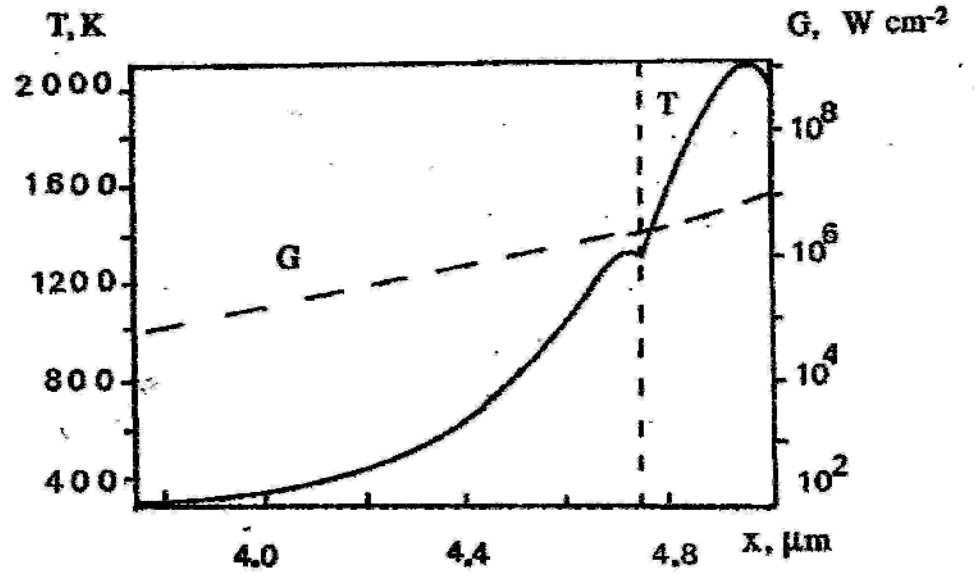

Fig. 2. The spatial temperature profile (solid line) *T(x)* and intensity of the radiation (dashed line) *G(x)* correspond to the developed evaporation. The vertical line corresponds to the position of the interface $x=\Gamma_{kv}(t)$.

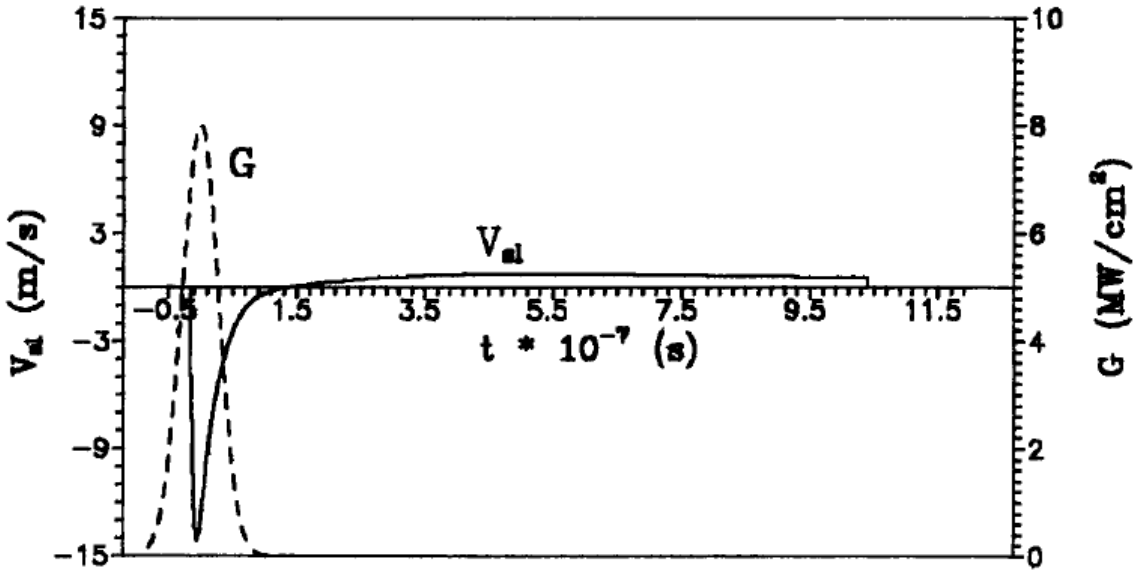

Fig. 3. Time dependence of melting velocity $\upsilon_{s\ell}$

The propagation velocities of the phase fronts at the same time increase sharply. Since the melting front velocity becomes comparable with the speed of sound in the solid phase $\upsilon_{s\ell} \le u_s$. Powerful flows of energy and matter through phase boundaries lead to a strong hydrodynamic perturbations. Under these conditions the classical Stephen model becomes unacceptable to describe the fast phase transitions and related processes.

The dynamics of fast heterogeneous phase transitions taking into account the rapid volumetric release of energy, a strong thermodynamic nonequilibrium and overheated metastable states can be described in terms of two-temperature hydrodynamic nonequilibrium Stefan-type model .[46-48]

Theoretical model. The laser radiation propagates from the right to the left and is partially absorbed at the surface of the metal target. Fig.4 shows spatial configuration of the phase fronts $\Gamma_{sl}(t), \Gamma_{l\upsilon}(t)$ and the shock wave in the condensed media $\Gamma_{sh,s}(t)$. The statement of the problem includes the following limitations and suppositions.

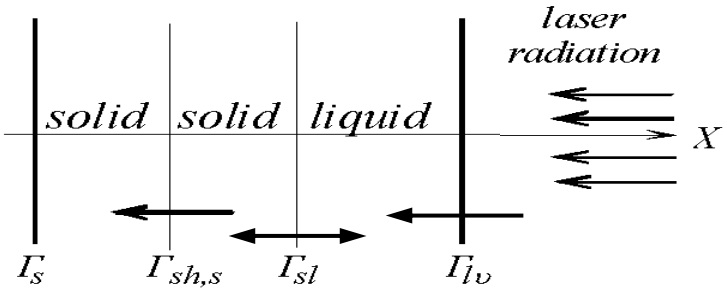

Fig. 4. Spatial phase configuration.

The mechanisms of the volume melting and evaporation are not included in the consideration. It is supposed that the melting front appear at the irradiated surface when the temperature reaches T_m and overheated metastable states behave in a stable way during the consideration.

The mathematical description and modeling of the pico- femtosecond laser melting of hard Aluminum target in vacuum is performed within the framework of following model:

$$\left(\begin{array}{l} \dfrac{\partial \rho}{\partial t} + \dfrac{\partial (\rho u)}{\partial x} = 0 \\ \dfrac{\partial (\rho u)}{\partial t} + \dfrac{\partial (\rho u^2)}{\partial x} = -\dfrac{\partial P}{\partial x} \\ \dfrac{\partial (\rho_e \varepsilon_e)}{\partial t} + \dfrac{\partial (\rho_e u \varepsilon_e)}{\partial x} = -\left(P\dfrac{\partial u}{\partial x} + \dfrac{\partial W_e}{\partial x} + g(T_e)(T_e - T_{ph}) + \dfrac{\partial G}{\partial x} \right) \\ \dfrac{\partial (\rho \varepsilon_{ph})}{\partial t} + \dfrac{\partial (\rho u \varepsilon_{ph})}{\partial x} = -\left(P\dfrac{\partial u}{\partial x} + \dfrac{\partial W_{ph}}{\partial x} - g(T_e)(T_e - T_{ph}) \right) \\ \dfrac{\partial G}{\partial x} + \alpha(T_e) G = 0, \qquad \rho_e = z\dfrac{m}{M}\rho, \end{array} \right)_k \tag{7}$$

$$-\infty < t < \infty, \qquad \Gamma_s < x < \Gamma_{sh,s}(t) \bigcup \Gamma_{sh,s}(t) < x < \Gamma_{s\ell}(t) \bigcup \Gamma_{s\ell}(t) < x < \Gamma_{\ell\upsilon}(t)$$

where $W_e = -\lambda(T_e, T_{ph})\dfrac{\partial T_e}{\partial x}$, $W_{ph} = -\lambda(T_{ph})\dfrac{\partial T_{ph}}{\partial x}$, $\varepsilon_e = C_{\upsilon e}(T_e)T_e$, $\varepsilon_{ph} = C_{\upsilon ph}(T_{ph})T_{ph}$

$$P(\rho,T)=P(\rho_e,T_e)+P(\rho_{ph},T_{ph})$$

Here: ρ, *u,* ε, *T*, *P* are the density, gas-dynamic velocity, internal energy and pressure, $\alpha(T_e), R(T_e)$ are the coefficient of volume absorption and the surface reflectivity, *G* is the laser radiation density, C_ϑ λ are the heat capacity and the heat conductivity coefficient, $g(T_e)$ is the electron-phonon coupling constant. The indexes *s*, *l,* υ represent solid, liquid and vapor phases, e, ph represent electron and phonon gas, $k = s, l$

The model of the surface non-equilibrium melting is formulated at the boundary $x=\Gamma_{s\ell}(t)$ as a set of three conservation laws: mass $j^m_{s\ell}$, momentum $j^i_{s\ell}$, energy $j^e_{s\ell}$ and an additional condition for temperature.

All relations are written in the coordinate system moving with the velocity of the solid phase u_s. The velocity of the phase front is given as $\upsilon_{sl}=\upsilon^*_{sl}-u_s$, where υ^*_{sl} is the velocity of the melting-crystallization front in the stationary (laboratory) coordinate system.

$$j^m_{s\ell}=\rho_s\upsilon_{s\ell}=\rho_\ell(u_s-u_\ell+\upsilon_{s\ell}), \tag{8}$$

$$j^i_{s\ell}=P_s+\rho_s\upsilon^2_{s\ell}=p_\ell+\rho_\ell(u_s-u_\ell+\upsilon_{s\ell})^2, \tag{9}$$

$$j^e_{s\ell}=-j^T_s+j^m_{s\ell}\left[H_s+\frac{\upsilon^2_{s\ell}}{2}\right]=-j^T_\ell+j^m_{s\ell}\left[H_\ell+\frac{(u_s-u_\ell+\upsilon_{s\ell})^2}{2}\right], \tag{10}$$

where $H_\ell=C_{ps}\Delta T_{s\ell}$ $H_\ell=C_{p\ell}\Delta T_{s\ell}+L_m$ $W_s=-\lambda(T_{ph,s})\dfrac{\partial T_{ph,s}}{\partial x}$, $W_\ell=-\lambda(T_{ph,\ell})\dfrac{\partial T_{ph,\ell}}{\partial x}$

Here H_s, H_ℓ, W_ℓ, W_s are the enthalpy and the heat flows in the solid and liquid phases correspondingly.

The energy conservation law for $j^e_{s\ell}$ can be easily transformed into canonical form of the differential Stefan condition:

$$\left(\lambda_{ph}\frac{\partial T_{ph}}{\partial x}\right)_s-\left(\lambda_{ph}\frac{\partial T_{ph}}{\partial x}\right)_\ell=\rho_s L^{ne}_m\upsilon_{s\ell}, \tag{11}$$

The differential Stefan condition is supplemented by the kinetic condition to obtain melting front velocity $\upsilon_{s\ell}$

$$\upsilon_{sl}(\Delta T_{sl})=\alpha\upsilon_h\left[1-\exp\left(-\frac{L^{ne}_m}{k_B T_m}\frac{\Delta T_{sl}}{T_{sl}}\right)\right] \tag{12}$$

where $T_{s\ell}=T_s=T_\ell=T_m(P_s)$, $T_m(P_s)=(T_{m,0}+\theta\cdot P_s)$, θ is a constant depending on the material, P_s is the pressure on the surface of the solid phase. The pressure dependence of the melting temperature is typical for the fast phase transitions where the velocity of the phase front υ_{sl} is comparable to the velocity if sound in the condensed media. L^{ne}_m is the non-equilibrium melting heat.

$$L_m^{ne} = L_m + \Delta C_{ps\ell}\Delta T_{s\ell} + \frac{\rho_s + \rho_\ell}{\rho_s - \rho_\ell}\frac{(u_s - u_\ell)^2}{2}, \quad \Delta C_{ps\ell} = (C_{p\ell} - C_{ps}), \quad \Delta T_{s\ell} = (T_m(P_s) - T_m)$$

The following relations are written for the electron component at $x = \Gamma_{sl}(t)$:

$$\left(\lambda_e \frac{\partial T_e}{\partial x}\right)_s = \left(\lambda_e \frac{\partial T_e}{\partial x}\right)_\ell, \qquad T_{e,s} = T_{e,\ell}, \tag{13}$$

The model of surface non-equilibrium evaporation is formulated within the approximation of the Knudsen layer. Three conservation laws are written at the boundary $x = \Gamma_{k\upsilon}(t)$: mass $j_{k\upsilon}^m$, momentum $j_{k\upsilon}^i$, energy $j_{k\upsilon}^e$ and two additional relations, characterizing the degree of non-equilibrium of the phase transition. All relations at the evaporating surface are written in the coordinate system moving with the velocity of the condensed phase $\upsilon_{k\upsilon} = \upsilon_{k\upsilon}^* - u_k$, $\upsilon_{k\upsilon}^*$ is the evaporation front velocity in the stationary (laboratory) coordinate system:

$$j_{k\upsilon}^m = \rho_k \upsilon_{k\upsilon} = \rho_\upsilon (u_k - u_\upsilon + \upsilon_{k\upsilon}), \tag{14}$$

$$j_{k\upsilon}^i = P_k + \rho_k \upsilon_{k\upsilon}^2 = p_\upsilon + \rho_\upsilon (u_k - u_\upsilon + \upsilon_{k\upsilon}),^2 \tag{15}$$

$$j_{k\upsilon}^e = -W_k + j_{k\upsilon}^m \left[H_k + \frac{\upsilon_{k\upsilon}^2}{2}\right] = -W_\upsilon + j_{k\upsilon}^m \left[H_\upsilon + \frac{(u_k - u_\upsilon + \upsilon_{k\upsilon})^2}{2}\right], \tag{16}$$

where $W_k = -\lambda(T_{ph,k})\frac{\partial T_{ph,k}}{\partial x}$, $W_\upsilon = -\lambda(T_\upsilon)\frac{\partial T_\upsilon}{\partial x}$, $H_k = C_{p\upsilon}(T_{ph,k} - T_b)$, $H_\upsilon = C_{p\upsilon}(T_\upsilon - T_b) + L_\upsilon$.

The conservation law can be finally written as

$$\left(\lambda_{ph} \frac{\partial T_{ph}}{\partial x}\right)_k = \rho_k \upsilon_{k\upsilon} L_\upsilon^{ne}, \tag{17}$$

$$L_\upsilon^{ne} = L_\upsilon(T_{ph,k}) + C_{p\upsilon}(T_b - T_{ph,k}) + \frac{\rho_k + \rho_\upsilon}{\rho_k - \rho_\upsilon}\frac{(u_\ell - u_\upsilon)^2}{2}$$

The values of $T_\upsilon, \rho_\upsilon, p_\upsilon$ are determined from the relations at the non-equilibirum Knudsen layer (6) where L_υ^{ne} is the non-equilibrium heat of evaporation , α_T, α_ρ are the Crout coefficients, M is the Mach number at the outer side of the Knudsen layer, ρ_{sat}, P_{sat} are the density and pressure of the saturated vapor, P_b, T_b, are the equilibrium boiling pressure and temperature, T_υ, ρ_υ are the vapor temperature and pressure. At M=1: $T_\upsilon = 0.633\ T_\ell$, $\rho_\upsilon = 0.328\ \rho_{sat}$.

The following relations are written for the electron component and the equation of the laser energy transfer at the boundary $x = \Gamma_{\ell\upsilon}(t)$:

$$-\lambda_e \frac{\partial T_e}{\partial x} = \sigma T_e^4, \quad G(t) = A(T_e)\cdot G_0 \exp\left(-\left(\frac{t}{\tau}\right)^2\right) \tag{18}$$

where σ is the Stefan-Boltzmann constant, R is the surface reflectivity coefficient. The temperature dependencies of the transport and optical properties $\lambda_e(T_e, T_{ph})$, $\lambda_{ph}(T_{ph})$, $g(T_e)$, $\alpha(T_e)$, $A(T_e)$ were determined using the approach from Refs.[47]

Modeling results. The surface of the Aluminum target in vacuum is irradiated by a laser pulse with Gaussian time distribution of intensity $G_k = A(T_k)G_0\, exp\left(-\left(\frac{t}{\tau}\right)^2\right)$, wavelength $\lambda = 0.8\,\mu m$, fluence of $F = 1.\,J\,cm^{-2}$, duration of $\tau = 10^{-12}$ s, $\tau = 10^{-15}\,s$, and peak intensity of $G_0 = F/\left(\pi^{1/2}\tau\right) = 5.64\cdot 10^{11} Wcm^{-2}$, . $G_0 = F/\left(\pi^{1/2}\tau\right) = 5.64\cdot 10^{14} Wcm^{-2}$

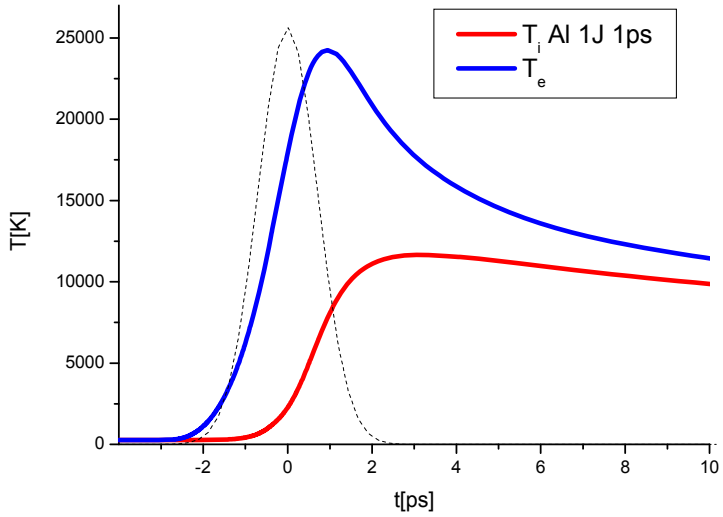

Fig. 5. Time dependence of electron and lattice temperatures on the target surface, (τ = 1 ps).

The main features of ultrashort laser influence determined by one of the major factors - a high rate of energy release. Fig. 5,7 show the time dependence of the temperature on the surface $T_e(t)$, $T_{ph}(t)$ for the picosecond and femtosecond pulses, respectively. Fig. 6,8 present the spatial distribution of temperature at maximum overheating of lattice for both duration of incident pulses. The time profiles $T_e(t)$ with a slight shift repeated time shape of the pulse, reaching the maximum values immediately after the peak intensity $T_{e\,max}(t) \approx 2.58\cdot 10^4\,K$, Fig. 5, for picosecond pulse and $T_{e\,\max}(t) \approx 5.48\cdot 10^4\,K$ for femtosecond, Fig. 7.

The maximum value of the lattice temperature is reached in the picosecond range and amounts $T_{ph,max} \approx 1.05\cdot 10^4\,K$ for picosecond pulse, Fig. 6, and $T_{ph,max} \approx 1.14\cdot 10^4\,K$ for femtosecond duration, Fig. 8. The ability to achieve such temperatures with femtosecond heating has been shown in [49] using molecular dynamic simulations.

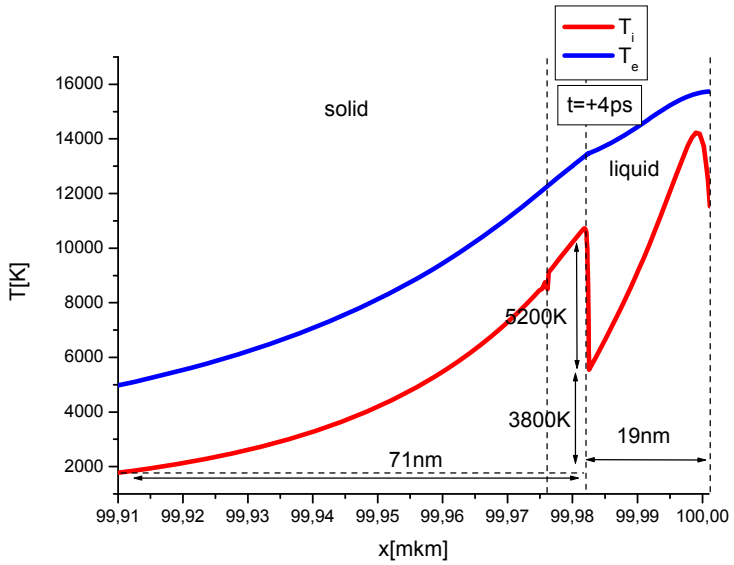

Fig. 6. Picosecond influence (τ = *1 ps*). Spatial distribution of electron and lattice temperatures at the moment t = *4 ps*.

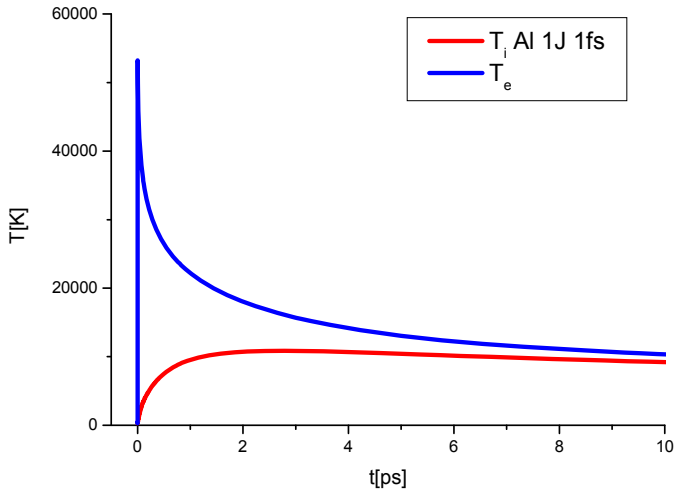

Fig. 7. Time dependence of electron and lattice temperatures on the target surface, (*τ=1fs).*

High heating rate predetermines high velocity of propagation of the phase fronts of melting $\upsilon_{s\ell}(t)$ and evaporation $\upsilon_{\ell\upsilon}(t)$. At picosecond influence melting begins at the leading edge of the laser pulse and quickly reaches a maximum value $\upsilon_{s\ell\,max}(t) \approx 4.25\ km/s$. Surface evaporation begins with some delay because of the larger quantity of specific energy of evaporation L_{υ}^{ne} ($L_{\upsilon}^{ne} >> L_{m}^{ne}$), maximum surface evaporation rate of about an order of magnitude less than the rate of melting $\upsilon_{\ell\upsilon\,max}(t) \approx 300\ m/s$. At femtosecond influence phase transformations begin with a big delay relative to the pulse ends after about $10^3\tau$.

High velocity of propagation of the phase fronts are associated with a powerful cross-flow of matter and energy across the interface. Combined with volumetric nature of the energy

transfer from the electron gas to the lattice, this leads to the formation of strongly overheated metastable states and the appearance of subsurface temperature maxima in the solid and liquid phases, Fig. 6,8. Since the maximum value of the velocity of the melting front are comparable to the speed of sound in the solid phase $\upsilon_{s\ell\,max}(t) \approx \upsilon_{sound}$ was formed a shock wave running ahead of the melting front, Fig. 6,8.

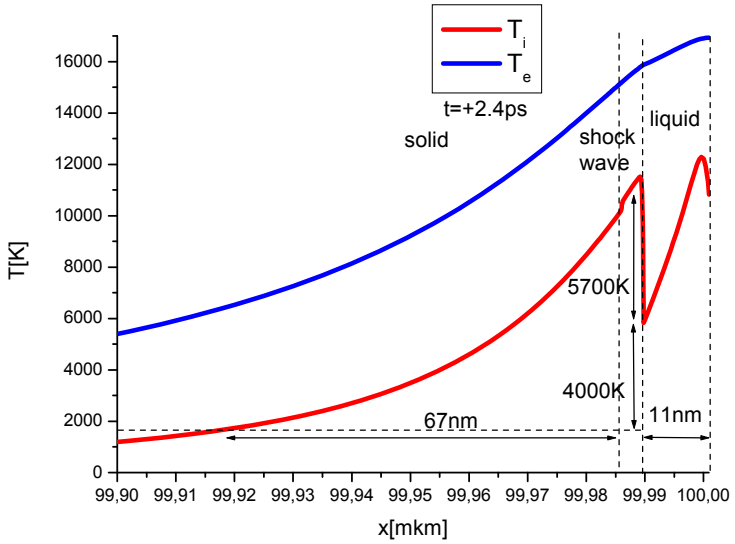

Fig. 8. Femtosecond influence ($\tau = 1$ *fs*). Spatial distribution of electron and lattice temperatures at the moment $t = 2.4$ *ps*

Location of phase fronts and shock wave are marked by vertical dashed lines. Arrows indicate the position of the maxima of temperature and their values. Let us remind that the maximum values of temperature maxima were obtained assuming no homogenous phase transitions whose description in the framework of continuum models is not possible, so the questions of the maximum overheat, of the stability of superheated states and of effective criterion of appearance of a new phase in a volume of superheated material in the process of nonequilibrium heating remain open. For their investigation requires the use of atomistic models and molecular dynamics methods.[50-52]

4 LIQUID-VAPOR TRANSITION

In continual approach this transition can be described in the framework of generalized Stefan model with sharp liquid-vapor interfaces where kinetic boundary conditions are formulated for mass, momentum and energy fluxes or its thermodynamic counterparts with addition of flow and phase front velocities.[43,53]

This model, incorporated in the whole set of gas- and hydrodynamic equations, makes it possible to investigate, e.g., stability problem of the evaporating surface at different values of vapor flow Mach number[53]. It permits also to investigate plasma formation in vapor plume provided ionization and recombination processes as well as other radiation effects are taken into account.[54-56]

Here for simplicity we consider only one equation of the set which describes temperature distribution in absorbing condensed matter ($x > 0$) subject to intense laser irradiation

$$\frac{\partial T}{\partial t} - \upsilon \frac{\partial T}{\partial x} - \chi \frac{\partial^2 T}{\partial x^2} = \frac{\alpha I}{\rho c} exp(-\alpha x) \tag{19}$$

$$x = 0: \quad c\chi \frac{\partial T}{\partial x} = L\upsilon; \qquad x = \infty: \quad T(t,\infty) = T_\infty$$

where the density ρ, heat capacity c, thermal diffusivity χ and absorption coefficient α are assumed to be constant. Boundary condition for the temperature gradient is formulated at the evaporating surface moving into the irradiated target with velocity χ**.** Vaporization velocity υ and latent heat of evaporation L depend on the surface temperature T_s. Reference frame in eq. (19) moves together with evaporating front at $x = 0$.

From (19) it follows for the steady state temperature distribution (see, e.g.,[6]):

$$T_{st} = T_\infty + \Delta T\left[A \cdot exp(-\alpha x) + B \cdot exp\left(-\frac{\upsilon}{\chi} x \right) \right] \tag{20}$$

$$A = \upsilon(c\Delta T + L)/c\Delta T(\upsilon - \alpha\chi),$$

$$B = 1 - A, \quad \Delta T = T_0 - T_\infty, \quad G = \rho\upsilon\left(L + c\Delta T\right) \tag{21}$$

$$\upsilon = 0.83 \frac{p}{\rho_0}\left(\frac{m}{2\pi k T_s} \right)^{1/2}, \quad p(T_s) = p_b \cdot exp\left[11.5 \cdot (1 - T_b/T_s)\right] \tag{22}$$

where $p(T_s)$, T_b and p_b = 1 bar are, respectively, saturated pressure, temperature and pressure at normal boiling point, m – vapor particle mass, k – Boltzmann constant. Coefficient 11.5 in (22) approximately describes saturated pressure behavior in the considered model. The considered model demonstrates that subsurface values of $T(x)$ can be higher than T_s if the parameter $y = \alpha\chi/\upsilon$ is not too big. It should be also reminded that during evaporation into vacuum the recoil pressure p_r is lower than saturated pressure $p\ (T_s)$. Due to this fact it is impossible to realize the steady state surface vaporization regime (20-22) when y is small or comparable with unity because of subsurface explosive boiling which can occur again and again during laser pulse action greatly disturbing .the surface vaporization regime (20-22) with only one plane phase boundary. Vaporization process in the case of bulk absorption was considered in several papers (see, e.g.,[6] and references therein) but some important features of the process still remain to be investigated experimentally and theoretically. It seems possible, e.g., that the features can manifest itself in destructive interference effect of simultaneous contributions from thermoacoustic and vaporization mechanisms to resulting pressure signals.[57,58]

For metals usually $y >> 1$ so that the steady state surface vaporization regime (20) has a rather wide applicability limits. In this situation, however, another question arises which also concerns the subsurface explosive boiling. Can this process develop in metals where $y >> 1$, temperature maximum T_m exceeds T_s only slightly and the distance T_m subsurface location from the surface is of the order of radiation penetration length (about 10 nm).

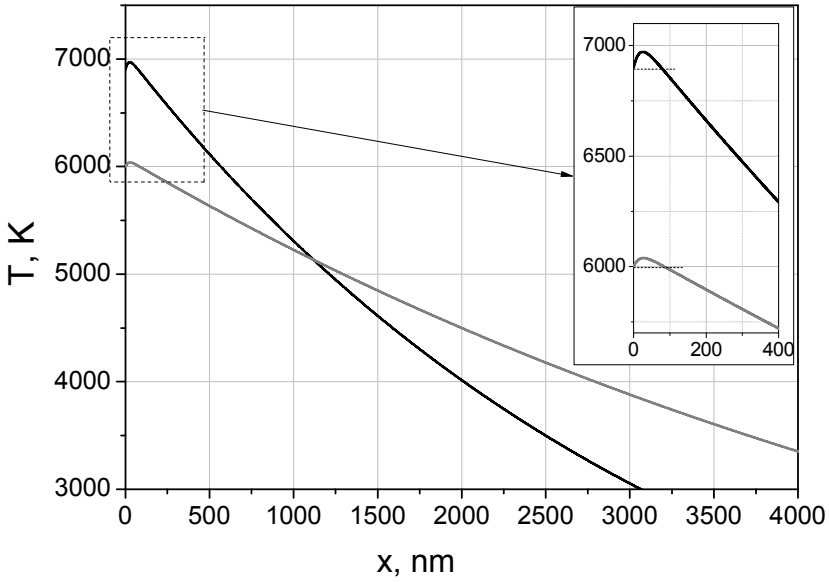

Fig.9. Temperature distributions T(x) for two laser intensities: G=19.5 MW/cm^2 (grey curve), G = 38.5 MW/cm^2 (black curve). Radiation goes from the left

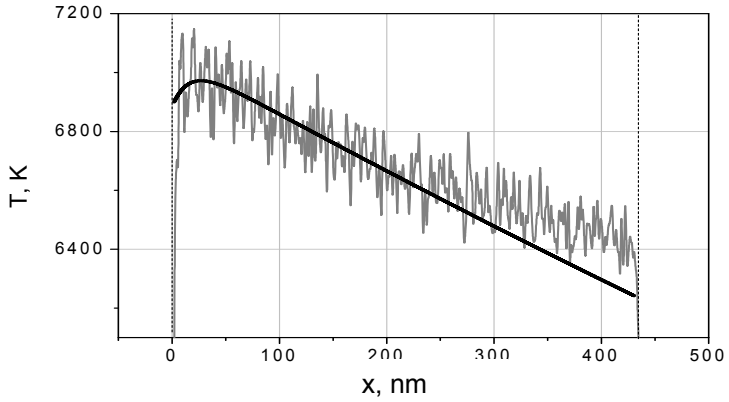

Fig.10. Comparison of temperature distributions from MD calculations (fluctuating curve).just before explosive boiling and from Stefan-like model (19) for G = 38.5 MW/cm^2. Radiation goes from the left

Negative answer to this question is given in recent paper[12] with references to some earlier works[4,7] where the explosive boiling problem was discussed in the continual approach framework. On the contrary, about four decades ago it was suggested that repetitive explosive boiling due to the subsurface superheating in metals should occur and the difference $\delta T = T_m - T_s$ should be taken into account despite its rather small value.[3] Such suggestion is in agreement with recent MD calculations.[9,10]

Fig 9 shows typical steady state temperature distribution in metal with parameters corresponding to the model used in [9,10]. In accordance with above mentioned temperature distribution features for metals the difference δT is hardly visible in Fig 9 except for the given inset. Nevertheless, it is the difference δT that gives rise to some remarkable aspects of explosive boiling process investigated in [9,10].with the help of MD modeling.

In [9,10] nanosecond laser ablation of liquid metal film (Al, 500 nm thickness) was studied in the intensity range 38.5 – 154 MW/cm^2 . In this range four different ablation regimes can be observed surface evaporation, explosive boiling, spinodal decomposition and supercritical fluid expansion.

In Fig. 10 two temperature distributions obtained from continual model (19) and MD calculations (fluctuating curve) are compared. Near the right film side the fluctuating curve goes somewhat higher than the continual model curve which corresponds to infinite film thickness value. Explosive boiling begins in the region of Tm location where vapor cavity appears and short (subnanosecond) pressure pulse is generated. Expansion of the subsurface cavity pushed the thin liquid layer (about 10 nm) away from the irradiated surface and afterword the process is repeated as it is seen from the density distribution in Fig 11. Such explosions occur at t = 1 ns, 1.4 ns, 1.6 ns, 2 ns and 2.3 ns after the constant radiation intensity G=38.5 MW/cm^2 is switched on at t = 0.

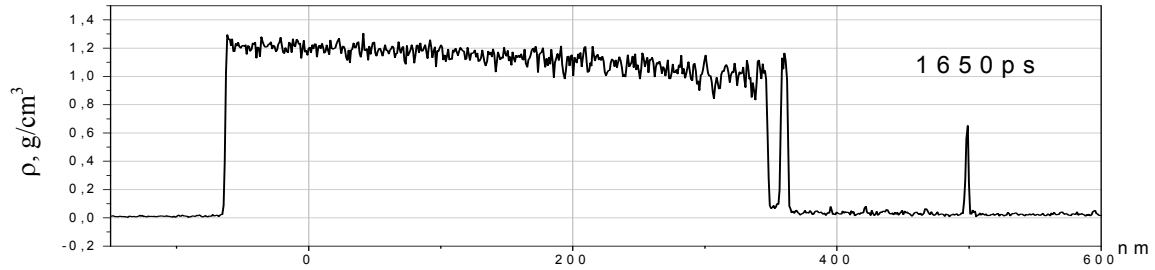

Fig.11. 1D particle density distribution at t = 1.65 ns after the radiation pulse with constant intensity G=38,5MW/cm^2 is switched on. Radiation goes from the right.

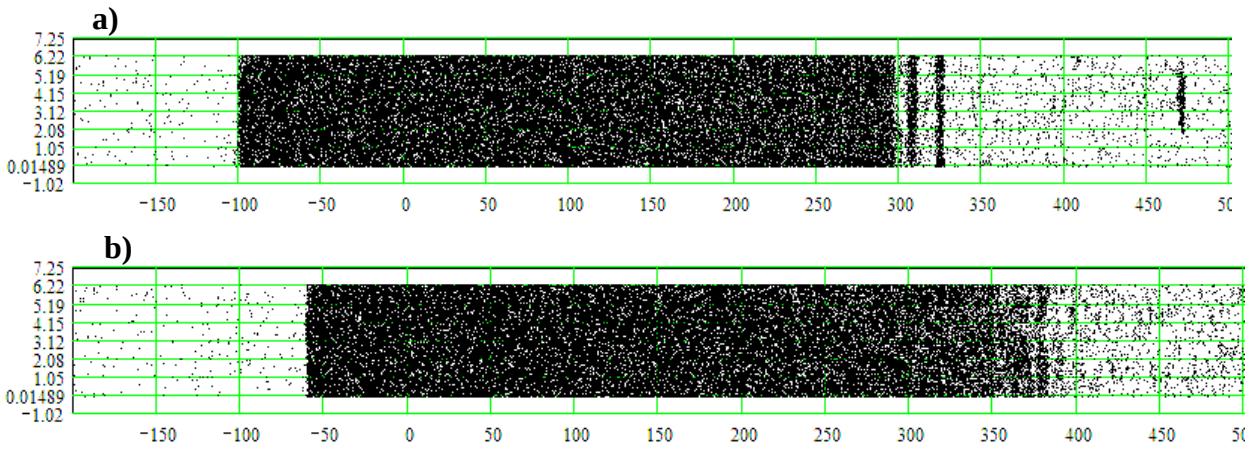

Fig.12. 2D snapshots of particle density at t = 1.82 ns after the radiation pulse with constant intensity G = 44 MW/cm^2 is switched on (a), and at t =0.73 ns with G= 88 MW/cm^2 (b) Radiation goes from the right.

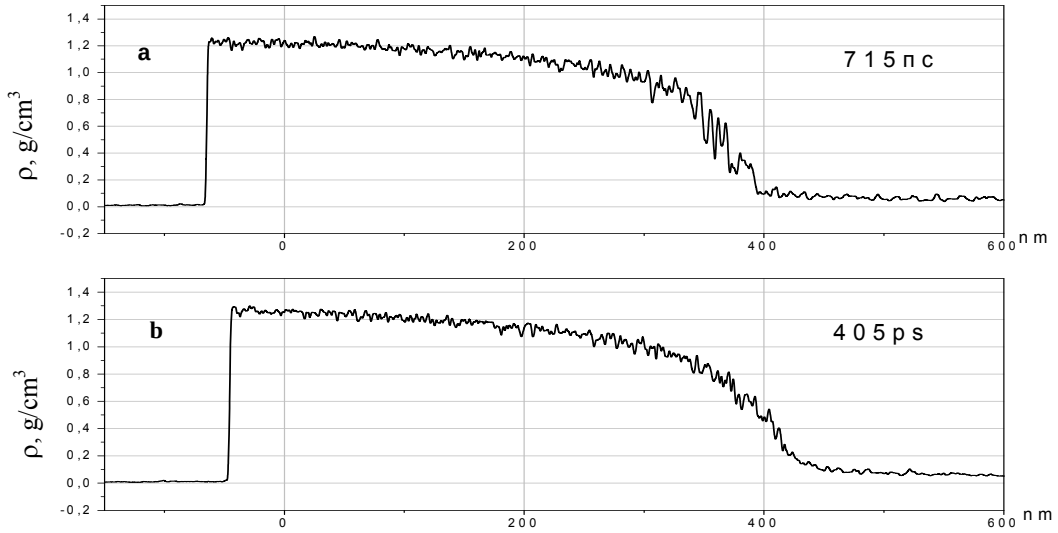

Fig.13. 1D particle density distributions at t = 0.715 (a, spinodal decomposition) and 0.405 ns (b, supercritical expansion) after the radiation pulse with constant intensities G=88 and 154 MW/cm^2 are switched on, respectively. Radiation goes from the right.

More detailed picture of nanosecond metal ablation evolution which includes studies of surface evaporation, explosive boiling, spinodal decomposition and supercritical fluid expansion (Fig 11-13) can be found.[9,10] This picture is based on MD calculation results and differs from the previous continual model descriptions of laser ablation[4,5,12] where, in particular, the subsurface superheating was not taken into account properly.

5 CONCLUDING REMARKS

Presented here comparison of the results obtained in the framework of continual and MD calculations shows that the small subsurface temperature maximum is very important for adequate explosive boiling description as it was suggested early.[3] This temperature maximum determines the short (subnanosecond) pressure pulses which appear during explosive boiling process and which were not considered in the continual descriptions.[4,5,7,12] Such short pressure pulses can be used as experimental markers which demonstrate during laser ablation how the irradiated matter is close to its critical region. It is clear[10] that in this region one should also consider plasma formation effects on the laser ablation process.

According to Van der Waals equation of state constant pressure heat capacity diverges and changes its sign at spinodal line. In real physical systems no such well defined line exists because of growing unstable thermodynamic fluctuations. Our estimations[59] based on the results MD calculations[10] shows that heat conduction coefficient grows near superheating temperature limit. Spinodal and critical point manifestations in strongly nonequilibrium conditions of laser ablation need more experimental and theoretical investigations.

Acknowledgment. This work was partially supported by Russian Fund of Basic Research grant № 13-02-01129, № 13-07-00597, № 15-07-05025.

REFERENCES

[1] V. A. Batanov, F. V. Bunkin, A. M. Prokhorov and V. B. Fedorov. "Evaporation of metallic targets caused by intense optical radiation", *Soviet Physics JETP*, **36**, 311-322 (1973).

[2] F.W. Dabby, U.C. Paek "High-intensity laser-induced. Vaporization and explosion of solid material", IEEE J. of Quantum Electronics, 8, 106 – 111 (1972).

[3] A.A. Samokhin "Some aspects of the intense evaporation of condensed media by laser radiation" Sov. J. Quantum Electron. 4, 1144 (1975).

[4] A. Miotello, R. Kelly, "Critical assessment of thermal models for laser sputtering at high fluences" Appl.Phys. Lett., **67**(24), 3535-3537 (1995).

[5] A.Miotello, R. Kelly. "Laser induced phase explosion: new physical problems when a condensed phase approaches the thermodynamic critical temperature", Appl. Phys. A, **69**, S67 (1999).

[6] A.A.Samokhin, "First-order phase transitions induced by laser radiation in absorbing condensed matter", Proceedings of the Institute of General Physics Academy of Science of the USSR, Commack, New York, 13, 1-161, 1990.

[7] N.M. Bulgakova, A.V. Bulgakov, "Pulsed laser ablation of solids: transition from normal vaporization to phase explosion", Appl .Phys. A, **73**, 199-208 (2001).

[8] . C. Wu, L.V Zhigilei, "Microscopic mechanisms of laser spallation and ablation of metal targets from large-scale molecular dynamics simulations", Appl. Phys. A, 114, 11-32 (2014).

[9] V.I. Mazhukin, A.A. Samokhin, M.M. Demin, A.V. Shapranov, "Explosive boiling of metals upon irradiation by a nanosecond laser pulse", Quantum Electronics, 44(4), 283-285 (2014).

[10] V.I. Mazhukin, A.A. Samokhin, M.M. Demin, A.V. Shapranov, "Modeling of nanosecond laser vaporization and explosive boiling of metals", Mathem. Montisnigri, 29, 68 - 90 (2014).

[11] V.I. Mazhukin, A.A. Samokhin, A.V. Shapranov, M.M. Demin, "Modeling of thin film explosive boiling - surface evaporation and electron thermal conductivity effect", Mater. Res. Express, 2(1), 016402 (1-9) (2015).

[12] M.Q. Jiang, Y.P. Wei, G. Wilde, L.H. Dai, "Explosive boiling of a metallic glass superheated by nanosecond pulse laser ablation", Appl. Phys. Let, 106, 021904 (1-6) (2015).

[13] J. Stefan, "Ueber die Theorie der Eisbildung, insbesondere ueber die Eisbildung im Polarmeere", Ann. Physik Chemie, 42, 269–286 (1891).

[14] G. Lamé, B.P. Clapeyron, "Mémoire sur la solidification par refroidissement d'un globe liquide", Ann. Chimie Physique, 47, 250–256 (1831).

[15] H.S. Carslaw and J.C. Jaeger, Conduction of Heat in Solids, 2nd ed. New York: Oxford Univ. Press, (1959).

[16] P.V. Breslavskii`, V.I. Mazhukin, A.A. Samohin, "O gidrodinamicheskom variante zadachi Stefana dlia veshchestva v metastabil`nom sostoianii", Docl. AN SSSR, 320(5), 1088-1092 (1991).

[17] P.V.Breslavskii`, V.I. Mazhukin, "Algoritm chislennogo resheniia gidrodinamicheskogo varianta zadachi Stefana pri pomoshchi adaptiruiushchikhsia setok", Matematicheskoe modelirovanie, 3(10), 110-115 (1991).

[18] Ch.Charach, I. Rubinstein. "Pressure-temperature effect in planar Stefan problems with density change", J. Appl. Phys., 71(3), 1128–1137 (1992).

[19] E.E. Sliadnikov, I.Iu.Turchanovskii`, "Kineticheskaia model` neravnovesnogo fazovogo perehoda, stimulirovannogo vozdei`stviem teplovogo istochnika", Izvestiia vuzov. Fizika, **58**, 84-91 (2015).

[20] Y.S.Hwang, V.I.Levitas, "Phase field simulation of kinetic superheating and melting of aluminum nanolayer irradiated by pico- and femtosecond laser", *Applied Physics Letters*, **103**, 263107 (2013).

[21] J.I. Masters, "Problems of intense surface heating of a slab accompanied by change of phase", *J. Appl. Phys.*, **27**, 477-484 (1956).

[22] G.V.Gordeev, "Nizkochastotny`e kolebaniia plazmy`", *ZHE`TF,* **27**, 19-24 (1954).
[23] A.F. Alexandrov, L.S. Bogdankevich, A.A. Rukhadze, *Principles of Plasma Electrodynamics*, Shpringer Verlg, Hyidelberg,Chapt. 4,5,12, (1984).
[24] I.M.Lifshic, M.I.Kaganov, L.V.Tanatarov. "Relaksacija mezhdu ehlektronami i kristallicheskojj reshetkojj", *ZhEhTF*, **31**(8), 232-237 (1956).
[25] I.M.Lifshic I.M., M.I.Kaganov, L.V.Tanatarov, "K teorii radiacionnykh izmenenijj v metallakh", *Atomnaja ehnergija*, **6**, 391-402 (1959).
[26] S.I.Anisimov, B.L.Kapeliovich, T.L.Perel`man, "E`lektronnaia e`missiia s poverkhnosti metallov pod dei`stviem ul`trakorotkikh lazerny`kh impul`sov", *ZHE`TF*, **66**, 776-779 (1974).
[27] D.S. Ivanov, L.V. Zhigilei, "Combined atomistic-continuum modeling of short-pulse laser melting and disintegration of metal films", *Physical Review B*, **68**, 064114 (1-22) (2003).
[28] Wu Ch., Zhigilei L.V., "Microscopic mechanisms of laser spallation and ablation of metal targets from large-scale molecular dynamics simulations", *Appl. Phys. A*, **114**, 11–32 (2014).
[29] V.V.Zhakhovskii, N.A.Inogamov, Yu.V.Petrov, S.I.Ashitkov, K.Nishihara, "Molecular dynamics simulation of femtosecond ablation and spallation with different interatomic potentials", *Appl. Surf. Sci.*, **255(**24), 9592-9596 (2009).
[30] G.E.Norman, S.V.Starikov, V.V.Stegailov, I.M.Saitov, and P.A. Zhilyaev, "Atomistic Modeling of Warm Dense Matter in the Two-Temperature State", *Contrib. Plasma Phys.*, **53(**2), 129-139 (2013).
[31] J.Lipton, W.Kurz, and R.Trivedi, "Rapid dendrite growth in undercooled alloys", *Acta Metallurgica*, **35(**4), 957-964 (1987).
[32] J.R. Cahoon, "On the Atomistic Theory of Solidification", *Metallurgical and materials transactions A*, **34A**, 2683 – 2688 (2003).
[33] Y. Ashkenazy, R.S. Averback, "Kinetic stages in the crystallization of deeply undercooled body-centered-cubic and face-centered-cubic metals", *Acta Materialia*, **58**, 524–530 (2010).
[34] G.I.Kanel, S.V.Razorenov, V. E. Fortov, "Shock-wave compression and tension of solids at elevated temperatures: superheated crystal states, pre-melting, and anomalous growth of the yield strength", *J. Phys.: Condens. Matter*, **6**, S1007–S1016 (2004).
[35] G.I.Kanel, S.V.Razorenov, K.Baumung, J.Singer, "Dynamic yield and tensile strength of aluminum single crystals at temperatures up to the melting point", *J. Appl. Phys.*, **90**, 136–143 (2001).
[36] G.S.Sarkisov, S.E.Rosenthal, K.W.Struve, D.H.McDaniel, E.M.Waisman, P.V.Sasorov, "Joule energy deposition in exploding wire experiments", *AIP Conf. Proc*. *Dense Z-Pinches: 5th Intern. Conf. Dense Z-Pinches,* **651**(1), 213–216 (2002).
[37] G.E.Norman, V.V.Stegailov, A.A.Valuev, "Nanosecond electric explosion of wires: from solid superheating to nonideal plasma formation", *Contrib. Plasma Phys*., **43**, 384 –389 (2003).
[38] X. Xu, C. Grigoropoulos, R.E. Russo, "Measurements of solid/liquid interface temperature during pulsed excimer laser melting of polysilicon films", *Appl. Phys. Lett.*, **65(**14), 1745-1747 (1994).
[39] Q.S. Mei, K. Lu, "Melting and superheating of crystalline solids: from bulk to nanocrystals", *Progress* in *Materials Science*, **52**, 1175-1262 (2007).
[40] L.I.Rubinshtei`n, *Problema Stefana*, Riga: Zvai`gzne, (1967).
[41] V.I. Mazhukin, A.A. Samarskii, "Mathematical Modeling in the Technology of Laser Treatments of Materials. Review", *Surveys on Mathematics for Industry*, **4(**2), 85-149 (1994).
[42] D. Crout, "An application of kinetic theory to the problems of evaporation and sublimation of monoatimic cases", *J. Math. Phys.*, **15**, 1-54 (1936).
[43] V.I. Mazhukin, A.A. Samokhin, "Boundary conditions for gas-dynamical modeling of evaporation processes", *Mathematica Montisnigri*, **XXIV**, 8–17 (2012).

[44] V.I. Mazhukin, I. Smurov, C. Dupuy, D. Jeandel, "Simulation of laser induced melting and evaporation processes in superconducting", *J. Numerical Heat Transfer Part A*, **26**, 587-600 (1994).
[45] V.I. Mazhukin, I. Smurov, G. Flamant, C. Dupuy, "Peculiarities of laser melting and evaporation of superconducting ceramics", *J.Thin Solid Films*, **241**, 109-113 (1994).
[46] A.V. Mazhukin, V.I. Mazhukin, M.M. Demin, "Modeling of femtosecond laser ablation of Al film by laser pulses", *Applied Surface Science*, 257, 5443–5446 (2011).
[47] V.I. Mazhukin. *Kinetics and dynamics of phase transformations in metals under action of ultra-short high-power laser pulses*. *Chapter 8*, Laser Pulses – Theory, Technology, and Applications, InTech, Croatia, ISBN 978-953-51-0796-5, 219-276 (2012).
[48] V.I. Mazhukin, M.M. Demin, A.V. Shapranov, "High-speed laser ablation of metal with pico- and subpicosecond pulses", *Applied Surface Science*, **302**, 6–10 (2014).
[49] Ch. Cheng, X. Xu, "Mechanisms of decomposition of metal during femtosecond laser ablation", *Physical Review B*, **72**, 165415(1-15) (2005).
[50] S. Plimpton, "Fast Parallel Algorithms for Short-Range Molecular Dynamics". *J. Comput. Phys*. **117(**1), 1–19 (1995).
[51] H. Zhang, M. Khalkhali, Q. Liu, J. F. Douglas, "String-like cooperative motion in homogeneous melting", *J. Chemical Physics*, **138**, 12A538(1 -16) (2013).
[52] Y. Gan, J. K. Chen. "Nonequilibrium phase change in gold films induced by ultrafast laser heating", *Optics Letters*, **37(**13), 2691 – 2693 (2012).
[53] I.N. Kartashov, A.A. Samokhin, I. Yu. Smurov, "Boundary conditions and evaporation front instabilities", *J. Phys. D: Appl. Phys*. **38**, 3703-3714 (2005).
[54] V.I. Mazhukin, I. Smurov, G. Flamant, "2D-simulation of the system: laser beam + laser plasma + target". *Applied Surface Science*, **96-98**, 89-96 (1996).
[55] V.I. Mazhukin, V.V. Nossov, I. Smurov, "Modeling of plasma-controlled surface evaporation and condensation of Al target under pulsed laser irradiation in the nanosecond regime", *Applied Surface Science*, **253**, 7686 – 7691 (2007).
[56] V.I. Mazhukin, A.V. Mazhukin, M.G. Lobok, "Comparison of nano- and femtosecond laser ablation of aluminium", *Laser Physics*, **19(**5), 1169 - 1178 (2009).
[57] V.I. Mazhukin, A.V. Shapranov, A.A. Samokhin, A.Yu. Ivochkin, "Mathematical modeling of non-equilibrium phase transition in rapidly heated thin liquid film", *Mathem. Montisnigri*, **27**, 65-90 (2013).
[58] A.A. Samokhin and N.N. Il'ichev, *Laser-induced photoacoustic and vaporization pressure signals in absorbing condensed matter: new results,* Phase Transitions Induced by Short Laser Pulses, New-York: Nova Publishers, (2009) ISBN 978-1-60741-590-9.
[59] A.A. Samokhin, P.A. Pivovarov, "On spinodal manifestation during fast heating and evaporation of heated thin liquid film", *Mathem. Montisnigri*, **33,** 108-111 (2015).

The results were presented at the thirteenth international seminar "Mathematical models & modeling in laser-plasma processes & advanced science technologies" (May 30 - June 6, 2015, Petrovac, Montenegro).